Vacuum current emission and initiation in an LaB_6 hollow cathode

BARCELO RENACIMIENTO HOTEL, SEVILLE, SPAIN / 14–18 MAY 2018

M. Praeger[(1)], A. Daykin-Iliopoulos[(2)], S. Gabriel[(3)]

[(1)]University of Southampton, Hampshire, U.K., SO17 1BJ, Email: mattp@soton.ac.uk
[(2)]University of Southampton, Hampshire, U.K., SO17 1BJ, Email: Alexander.Daykin-Iliopoulos@soton.ac.uk
[(3)]University of Southampton, Southampton, U.K., SO17 1BJ, Email: sbg2@soton.ac.uk

KEYWORDS: LaB_6, krypton, pre-ignition current, hollow cathode.

ABSTRACT:

This paper presents the first investigation of pre-ignition currents and the ignition process in an LaB_6 hollow cathode running on krypton propellant. Vacuum and pre-ignition currents are found to be consistent with space charge limited behaviour. A novel, low power ignition strategy with the potential to reduce insert and orifice erosion is also shown.

1. INTRODUCTION:

The initiation of LaB_6 hollow cathodes needs higher temperatures and perhaps higher keeper voltages than BaO cathodes due to the higher work function of LaB_6 compared to BaO. Actual heater power levels, time to initiation and ignition voltages will depend on the details of the cathode design, including geometry (e.g. orifice diameter, keeper cathode separation) and thermal design [1]. Despite these parametric dependencies, a complete understanding of the detailed mechanisms involved in the initiation of LaB_6 cathodes is not available which makes reliable prediction of the required heater power and ignition voltage difficult; hence the sizing of the heater, the resulting start time and the ignition voltage (which impact upon keeper supply design) are essentially empirical in nature. Cathode temperature can be used as an indicator of when the cathode will ignite but since measurements of the cathode insert temperature are very difficult [2] especially with smaller cathodes, this methodology is again empirical and most likely rather uncertain, being dependent on the specific cathode design. It seems that there is no published systematic investigation of the ignition process of LaB_6 cathodes.

For BaO insert cathodes, the mechanism for initiation is generally accepted [3,4] and depends on the release of free barium which then migrates to the front surface of the cathode tip, forming a low work function layer which can then facilitate breakdown to the keeper. For LaB_6 cathodes, the mechanism cannot be the same but is probably related to the release of a certain minimum thermionic emission current from the insert surface (or part of it), the flow rate, the applied keeper potential and the keeper cathode separation.

This paper focuses on the measurement of the vacuum or pre-ignition current i.e. before gas flow initiation, which will depend on the insert temperature and work function, the hypothesis being that it is this parameter which governs whether or not ignition occurs. Additionally, measurements of the current immediately after ignition, at three different gas flow rates, are presented in order to demonstrate ignition.

2. EXPERIMENTAL APPARATUS

2.1. Electrical Apparatus

The electrical configuration of the experimental apparatus is shown schematically in Fig. 1. Power supplies manufactured by Elektro-Automatik are used, with separate supplies for the heater (EA-PS 2084-10B), keeper (EA-PS 9750-12) and anode (EA-PS 9200-70). The supplies are all computer controlled, with current and voltage data logged at approximately 0.4 s intervals.

Precise measurements of the current passing through the hollow cathode are made using an ammeter connected in series between the LaB_6 insert and the experiment ground. Two different instruments were utilised in this location: A Keithley 6485 picoammeter (used to measure pre-ignition currents of up to 20 mA) and a Thurlby Thandar Instruments 1604 multimeter (used to measure the larger post-ignition currents, up to 400 mA on the mA input and up to 10 A on the A input).

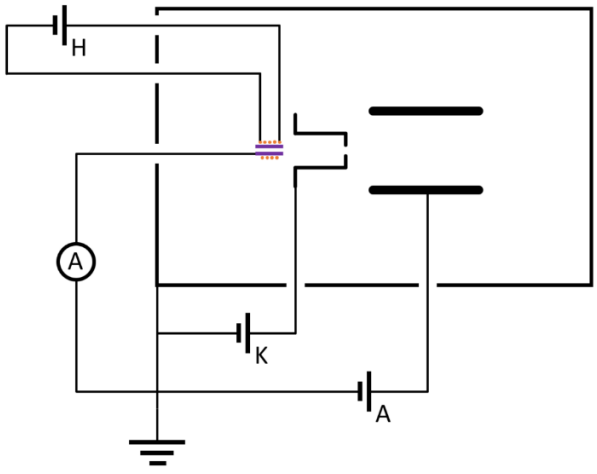

Figure 1. Electrical circuit used for current measurement experiments.

2.2. Gas and Pressure Control

Experiments are carried out in a cylindrical vacuum chamber (approximately 1.2 m in length and 0.6 m in diameter). Two large turbo pumps provide a combined pumping speed of 8600 L/s (N_2) and an ultimate pressure of 10^{-9} mbar and a background pressure of between 10^{-5} and 10^{-7} mbar depending on the mass flow rate. The turbos are backed by a large rotary pump. Chamber pressure is measured and logged using a calibrated, computer controlled, vacuum gauge (Kurt J. Lesker 354 Series Ion Gauge).

Propellant gas is delivered via a mass flow controller (Bronkhorst EL-Flow Select) capable of flow rates in the range 2-100 sccm. The mass flow rate is computer controlled and measured values are logged throughout the experiment.

2.3. Hollow Cathode

The cathode insert is a cylindrical tube of LaB_6. The insert is mounted in a metal tube which has provision to install plates with various orifice sizes at the downstream end. A resistive heating element (with is electrically isolated from both the cathode tube and the keeper) and multiple layers of thermal shielding are positioned between the cathode tube and the keeper. The keeper is machined from Poco graphite with an aperture of approximately 10 mm OD. The anode is a section of stainless steel tube 100 mm length and 100 mm in diameter, positioned 37 mm from the keeper. Ceramic materials are used to securely mount and electrically isolate the above components. The apparatus is shown in Fig. 2.

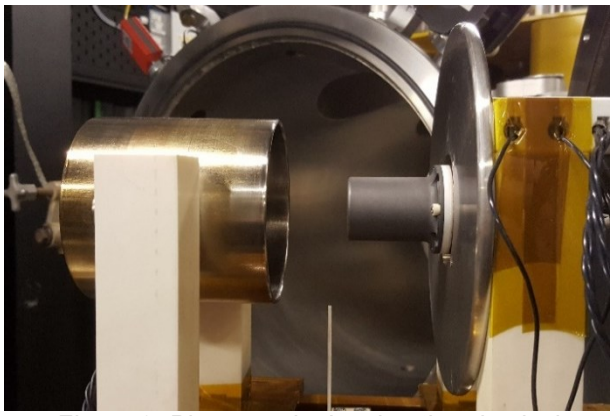

Figure 2. Photograph showing the physical arrangement of the anode and keeper.

3. EXPERIMENT PROCEDURE

Heater power, keeper and anode voltages and mass flow rate (of Krypton) are systematically varied over the ranges specified in Tab. 1.

The resulting cathode current is measured using either the picoammeter or multimeter depending upon the expected current magnitude. Each measurement is repeated three times to allow estimation of the error and to allow identification of any outliers.

Table 1. Range of experiment parameters tested.

	Min	Step	Max	Unit
Heater Power	0	10	150	W
Keeper Voltage	0	5	100	V
Anode Voltage	0	10	50	V
Kr Flow Rate	0	5	15	sccm

Care is taken to ensure that an adequate period of stabilisation is allowed at each position of the parameter sweep. This is particularly important in the case of changes to heater power as it is important that measurements are made under thermal equilibrium conditions. Delays of at least 17 minutes after each change in heater power, 1 minute after each change in mass flow rate and 10 seconds after each change in supply voltage are allowed prior to cathode current measurement. Observations made with a pyrometer indicate that it takes approximately 5 minutes for the temperature to stabilise after a 10 W change in heater power. The mass flow controller overshoots significantly but for a 5 sccm change it settles to the desired setpoint within 10 seconds. For a 5 V step change, the keeper power supply stabilises at the new value in less than 1 second. Fig. 3 provides an example section of the logged data and illustrates the experiment procedure.

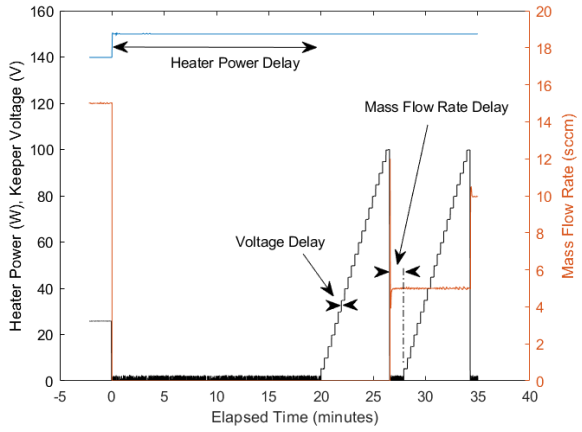

Figure 3. A section of logged data showing the delay times and the experiment procedure. Current measurements are made at each step in keeper voltage.

3.1. Defining Pre-Ignition and Ignition States

It is assumed that the hollow cathode discharge cannot be ignited in the absence of gas flow. The current measured with zero gas flow is therefore defined as the pre-ignition current. The value of pre-ignition current can therefore be measured for each combination of heater power, keeper and anode voltages.

When propellant gas is introduced, the measured current may conform to the pre-ignition current (in which case the hollow cathode is in a pre-ignition state). If the measured current deviates significantly from the pre-ignition value, the hollow cathode is considered to have ignited.

4. Results

4.1. Pre-Ignition Current (Picoammeter)

The first dataset records the vacuum, pre-ignition currents (i.e. the Kr mass flow rate is always set to 0 sccm). Since the hollow cathode will not ignite, the current flows are expected to be quite small. The picoammeter is therefore used for these measurements as it offers superior sensitivity and resolution.

Fig. 4 plots the measured current values on 3d axes in order to show the overall form of the pre-ignition current as a function of heater power and keeper voltage. This figure includes data recorded with 0 V and with 50 V applied to the anode. In our experiment geometry the anode voltage was found to have no effect on the pre-ignition current. This is presumably because the anode's effect on the electric field near to the insert is negligible (at least when 37 mm away and for up to 50 V).

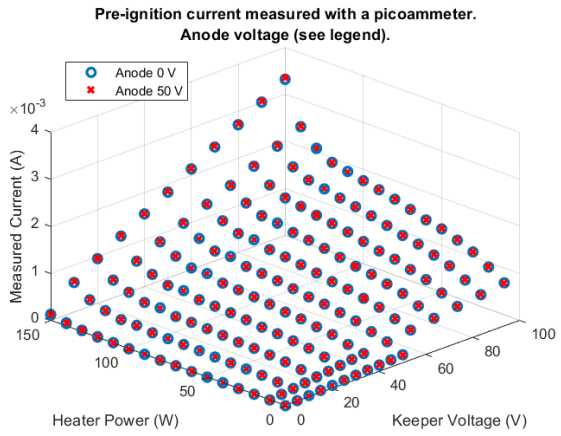

Figure 4. Pre-ignition current as a function of heater power and keeper voltage. Markers indicate anode voltage, blue circles 0V, red crosses 50 V.

For clarity, Figs. 5 and 6 plot the pre-ignition current values on conventional axes (for the anode = 0 V).

Fig. 5 shows that, for each heater power, the pre-ignition current increases smoothly as a function of keeper voltage. As heater power is increased, the gradient of the curve steepens so that a higher current is reached for the same keeper voltage. Increasing heater power from 140 W to 150 W causes a much larger change in gradient than the same 10 W step would cause at lower heater powers.

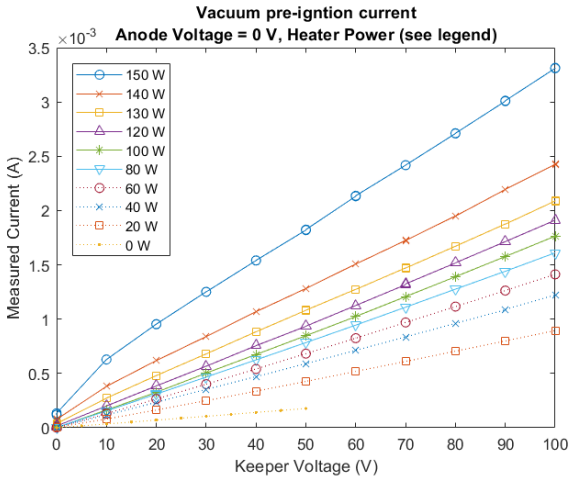

Figure 5. Pre-ignition current (measured with the picoammeter) as a function of keeper voltage at several different heater powers. Fixed anode voltage of 0 V.

Considering the response as a function of heater power (see Fig. 6); the steepening gradient that was observed in Fig. 5 is now clearly seen as a sharp increase in pre-ignition current for heater powers above 120 W. The measured current also increases quite rapidly at low heater powers which leads to the impression of a slight levelling off between 50 and 100 W of heater power.

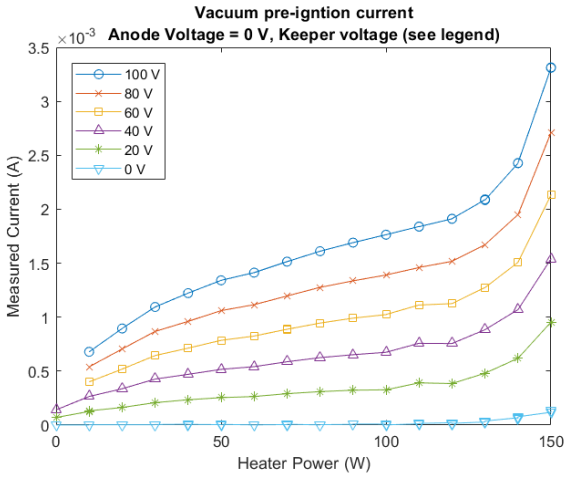

Figure 6. Pre-ignition current (measured with the picoammeter) as a function of heater power at several different keeper voltages. Fixed anode voltage of 0 V.

4.2. Pre-Ignition Current (Multimeter)

Large current flows during ignition could damage the picoammeter. The multimeter is therefore used for measurements with gas flow. This device has separate inputs for currents up to 400 mA and up to 10 A. Before proceeding to the gas flow measurements we must establish how each of these inputs resolves the pre-ignition current.

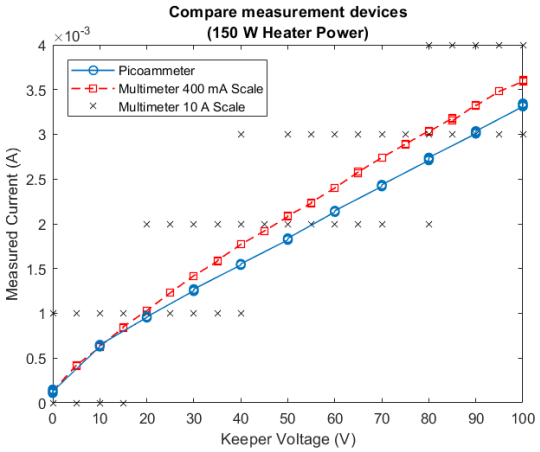

Figure 7. Pre-ignition current (measured with the multimeter mA input) as a function of heater power and keeper voltage for Kr flow rate of 0 sccm.

Fig. 7 shows very close agreement between the picoammeter and the 400 mA input of the multimeter. The only exception is that the multimeter is incapable of measuring the very low currents that occur at low heater power and low keeper voltages; these data are therefore truncated. The 10 A scale is limited to 1 mA resolution, however, the measured values clearly follow the same trend as the picoammeter data.

4.3. Ignition Current (400 mA Scale)

This dataset is recorded using the mA input of the multimeter, with the keeper current limit set at 0.35 A (to avoid exceeding the 400 mA capability of the device). The anode supply is not used in this dataset. These measurements employ Krypton flow rates of 0, 5, 10 and 15 sccm which allows a plasma to be ignited for higher heater powers. When ignition occurs the current increases rapidly until it reaches the current limit. At this point the keeper power supply automatically switches from voltage control mode to current control mode and remains at the current limit until the plasma is extinguished.

Figs. 8 and 9 show the result when Krypton propellant gas is introduced. For heater powers of up to 100 W the pre-ignition current is largely unchanged by the addition of propellant gas. Similarly, for keeper voltages of up to 30 V little change is observed.

For heater powers above 100 W with keeper voltages above 30 V a plasma is ignited. The measured current values (solid lines in Figs. 8 and 9) deviate significantly from the vacuum, pre-ignition values (dotted lines) and the current increases from a few mA to quickly reach the current limit of 350 mA.

Note that there are a few data points in Fig. 8 where ignition has occurred but the current remains below the 350 mA limit set on the keeper supply. This means that the supply is in voltage control mode and that the emitter is unable to provide any additional current under its present conditions.

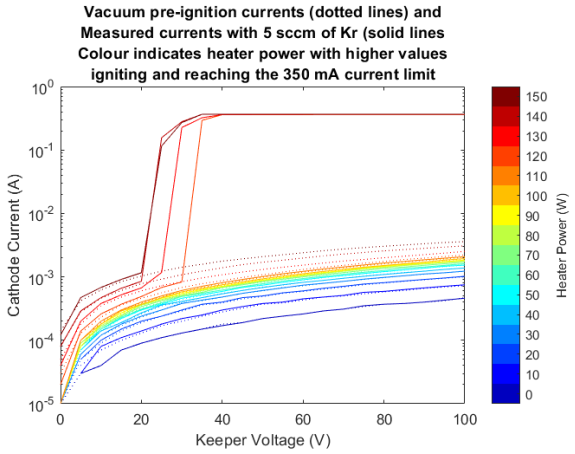

Figure 8. Measured current vs keeper voltage with a Kr flow rate of 5 sccm and a 350 mA keeper current limit. (Measured with the multimeter mA input and plotted on a logarithmic current scale).

Increasing the mass flow rate from 5 to 15 sccm has the effect of slightly reducing the requirements for ignition; allowing it to be achieved at 110 W of heater power rather than 120 W and at 20 V of keeper bias rather than 25 V.

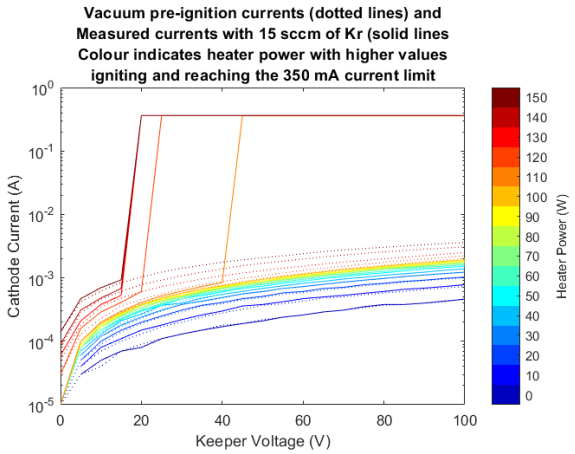

Figure 9. Measured current vs keeper voltage with a Kr flow rate of 15 sccm and a 350 mA keeper current limit. (Measured with the multimeter mA input and plotted on a logarithmic current scale).

4.4. Ignition Current (10 A Scale)

In the previous dataset the relatively small difference between the pre-ignition current (a few mA) and the current limit value (350 mA) made it difficult to observe intermediate ignition currents. (I.e. The current limit was reached almost immediately). In this dataset the multimeter A input is used allowing the keeper current limit to be increased to 5 A. This dataset covers only the higher heater powers where ignition is expected.

The results follow the same basic form as those obtained with the two other measurement systems. Due to the lower resolution of the high current input, the low current values are severely truncated. On the other hand, this input mode allows observation of larger currents that occur after ignition.

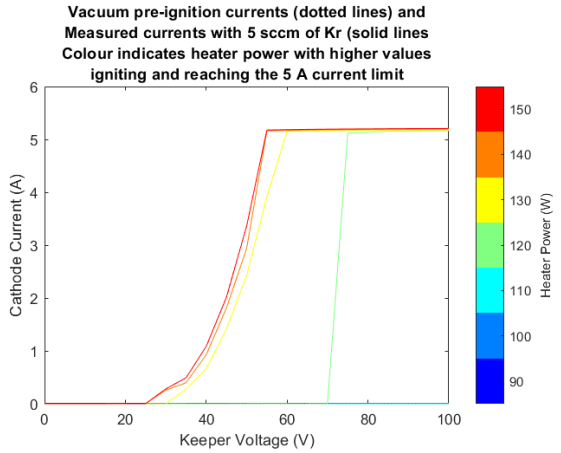

Figure 10. Pre-ignition current with a 5 A keeper current limit, as a function of keeper voltage for a Kr flow rate of 5 sccm. (Linear current scale).

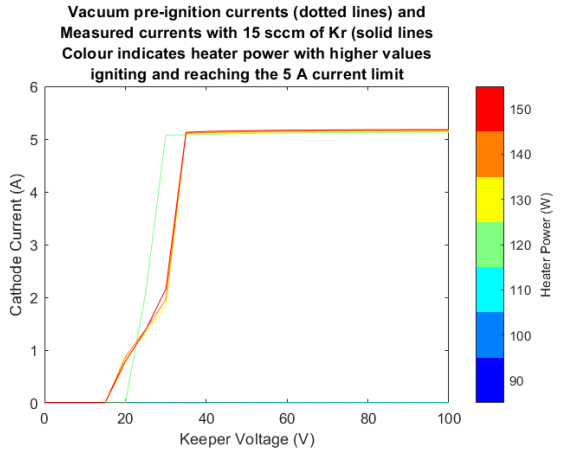

Figure 11. Pre-ignition current with a 5 A keeper current limit, as a function of keeper voltage for a Kr flow rate of 15 sccm. (Linear current scale).

Fig. 10 clearly shows several post-ignition current values that are intermediate between the pre-ignition current level (the baseline) and the keeper supply, current limit. These data points follow an upward sweeping curve with the measured current appearing to increase exponentially with keeper voltage.

In Fig. 11 at 15 sccm the increase in post-ignition current clearly occurs at a lower keeper voltage and at a faster rate.

Figs. 10 and 11 reveal that ignition can occur at very low keeper voltages (as shown in section 4.3) and that, once ignited, the keeper voltage may be increased until the desired current is achieved (or until the arbitrary current limit is reached).

4.5. Temperature Measurements

Theoretical calculations of the emitter current require knowledge of the emitter temperature. A hot wire pyrometer was therefore used to measure the temperate of the orifice plate as a function of heater power. This data is presented in Fig. 12.

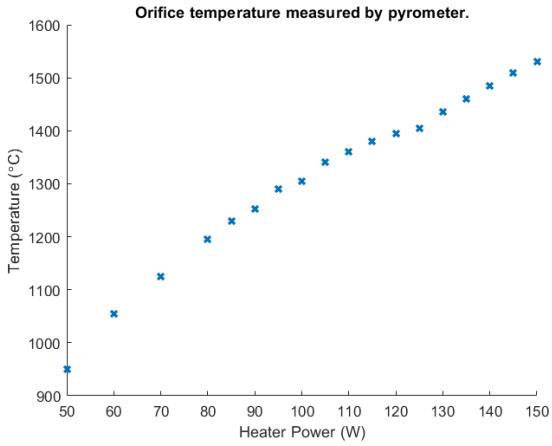

Figure 12. Orifice plate temperature vs heater power measured using a hot wire type pyrometer.

After reaching thermal equilibrium with the heater power set at 150 W the pyrometer reads 1530 °C. This value underestimates the emitter temperature because of transmission losses in the vacuum chamber viewport, material emissivity and thermal losses which cause the orifice plate to be cooler than the insert. Thermal modelling of the hollow cathode allow us to predict that at 150 W the actual insert temperature will be nearer to 1800 °C.

5. ANALYSIS

5.1. Vacuum Pre-Ignition Currents

Emitter current density is typically considered either to be space charge limited, in which case it is described by Child's law, or thermally limited and described by the Richardson equation [5].

In Child's law (Eq. 1) [6] the current density J_C is independent of emitter temperature and varies as the 3/2 power of applied voltage (V is the keeper voltage in the case of these experiments).

$$J_C = \frac{4\epsilon_0}{9d^2}\sqrt{\frac{2e}{m}}V^{\frac{3}{2}} \qquad (1)$$

Where ε_0 is the vacuum permittivity, e and m are the electron charge and mass and d is the electrode separation (cathode-keeper gap). Note: This equation is derived for a plane-plane electrode geometry, however, it serves as an initial estimate for currents produced in our hollow cathode setup.

The Richardson equation (Eq. 2) determines the current density (J_R) from the emitter temperature (T, in °K) and its work function (W, expressed in eV).

$$J_R = AT^2 e^{\left(\frac{eW}{k_B T}\right)} \quad (2)$$

A is the Richardson constant (Eq. 3), k_B is Boltzmann's constant and h is Planck's constant.

$$A = \frac{4\pi e m {k_B}^2}{h^3} \quad (3)$$

The Richardson equation can be modified to account for Schottky barrier lowering as a result of an applied field [1].

$$J_S = AT^2 e^{(\mu)} \quad (4)$$

where

$$\mu = \frac{-W - \sqrt{\frac{e^3 V}{4\pi\epsilon_0 d}}}{k_B T} \quad (5)$$

J_C, J_R and J_S are all current densities and so for comparison with the experimentally derived currents we must assume an emitter area. Fig. 13 shows the current predicted by Child's law for four different effective emitter areas.

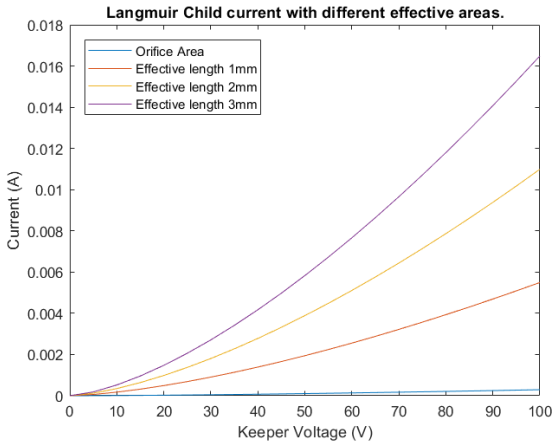

Figure 13. Current as a function of keeper voltage as predicted by Child's law (Eq. 1) for different effective emitter areas.

In section 4 we observed pre-ignition currents of up to 3.5 mA (for 100 V keeper and 150 W heater). In order to reach the experimentally observed value an effective emitter area of 6 mm^2 is required. This equates to a 0.6 mm length of the cylindrical inner surface of the insert (out of a total length of 15 mm).

In this calculation we take the emitter work function for LaB_6 to be 2.66 eV [7,8] which is consistent with the range of values reported in [9], however, here we neglect the material specific compensation term (D in [7]).

A similar calculation can be performed for the Richardson equation (Eq. 2) (see Fig. 14); under these conditions the effects of Schottky barrier lowering are very small and so these are not included in the plot. The same value for the work function of LaB_6 is used and the insert temperature is assumed to be as measured with the pyrometer. At a heater power of 150 W the orifice plate reached 1530 °C; at this temperature Eq. 2 predicts a current density of 14.6 A.cm^{-2}. If the insert emits from a 3mm length of its inner surface then the Richardson equation predicts a current of 4.1 A.

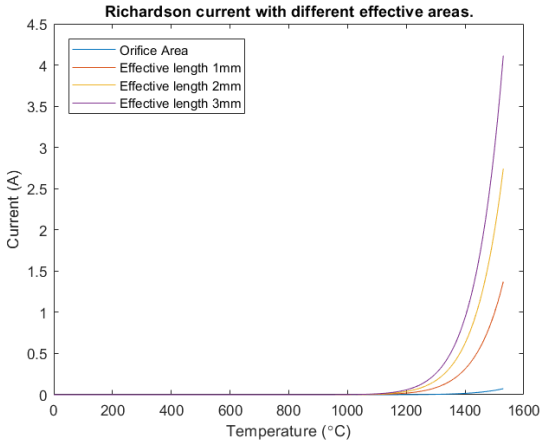

Figure 14. Current as a function of emitter temperature as predicted by the Richardson equation (Eq. 2) for different effective emitter areas.

In order for the Richardson equation to predict the experimentally observed current (3.5 mA at 150 W and 100 V) the effective area must be just 0.02 mm^2. This equates to a length of just 2.5 µm out of the emitters total length on 15 mm.

When current density is plotted against voltage, on log-log axes, Child's law appears as a straight line, rising with applied voltage. Richardson's equation produces a horizontal line (since it is independent of voltage); however, when Schottky barrier lowering is included this introduces a slight upward trend as voltage is increased (see Fig. 15).

The pre-ignition current data (from Fig. 5) at 50, 100 and 150 W heater power is converted from measured current to current density using the 6 mm^2 emitter area that was determined with the aid of Fig. 13. By plotting this data on the same axes as the theoretical curves for Child's law and the Richardson Schottky equation it becomes clear our pre-ignition currents are space charge limited.

As shown by Lin [5], the net current density (which is observed experimentally) is essentially determined by the lower of the two limits plotted in Fig. 15. In the region near to the intersection of these curves the actual current density value will be lower in order that there is a smooth transition

between the limits. This may explain the difference in gradient between the experimental data and the Child's law line. Lin finds that the effects of space charge extend well to the right of the intersection and into the region of higher applied voltage that is nominally termed thermally limited.

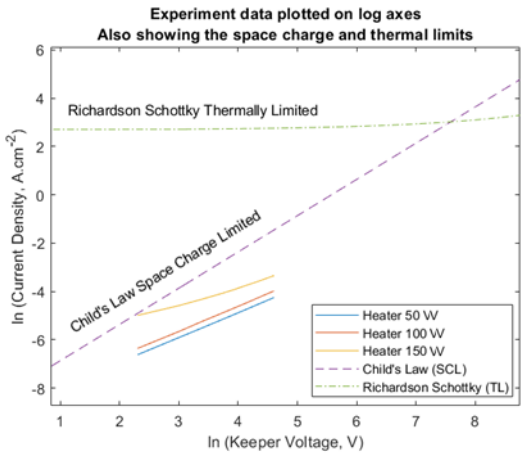

Figure 15. Current as a function of emitter temperature as predicted by the Richardson equation (Eq. 2) for different effective emitter areas.

5.2. Ignition Currents

In order to start the our hollow cathode in spot mode we would typically select a flow rate of 40 – 50 sccm, a keeper voltage of 100-150 V and a keeper current limit of 2 A. The results presented in sections 4.3 and 4.4 demonstrate ignition of the hollow cathode at Krypton flow rates and keeper voltages that are comparatively very low. Ignition of the hollow cathode was demonstrated with just 5 sccm of Kr, 25 V on the keeper and 140 W of heater power; or alternatively, with 35V and 120 W if lower heater power is preferred. Increasing the mass flow rate to 15 sccm allows for reduction in either the keeper voltage or heater power. At 15 sccm, ignition could be achieved with 20 V and 130 W or with 45 V and 110 W. In this low power starting mode it appears to be possible to trade-off heater power against flow rate and keeper voltage. This flexibility could potentially be of operational interest; for example, it could help in optimising hollow cathode operation to power supply capabilities and vice versa. Additionally, starting the hollow cathode at very low discharge power (although probably in plume mode) could potentially reduce emitter and orifice startup erosion by avoiding large transient currents which occur during ignition (even for spot mode).

Fig. 16 provides a more detailed view of the 5 sccm, 350 mA data (similar to Fig. 8 but plotted against heater power). With gas flow on, the last current value before ignition is typically just below 1 mA, however, whilst this condition may be necessary it does not seem to be sufficient. I.e. If the keeper voltage is not high enough (40 V or below in Fig. 16) ignition will not occur even though the pre-ignition current exceeds 1 mA.

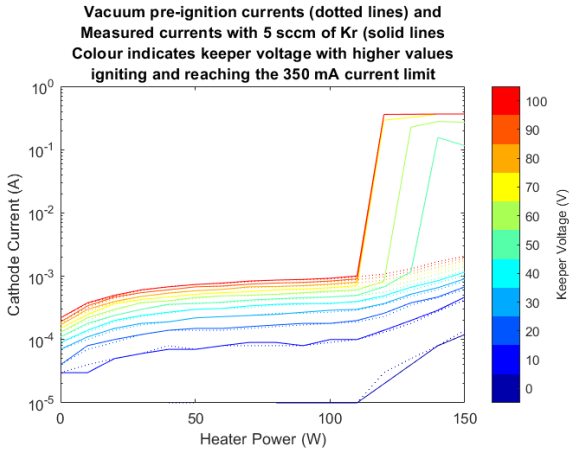

Figure 16. Dotted lines – vacuum pre-ignition current. Solid lines – current measured with 5 sccm of Kr (ignition is achiever for the higher heater powers and keeper voltages).

Brief tests were carried out to determine whether or not it was possible to ignite the hollow cathode in the low power mode described above and then to migrate to normal operation at higher current levels. It was found that with the keeper set at 27 V and a Kr flow rate of 15 sccm, once ignited and at the current limit of 350 mA, raising the current limit to 9.5 A caused the keeper supply to revert to voltage control mode; the new current limit was not reached (see Fig. 17).

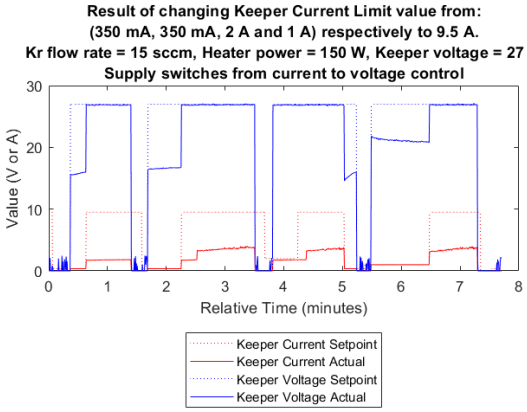

Figure 17. Hollow cathode is ignited with a 350 mA current limit which is then increased to 9.5 A. With a keeper voltage of 27 V the supply reverts to voltage control mode.

In contrast, with the keeper set at 30 V, when the keeper current limit was increased from 350 mA to 9.5 A, the keeper current increased within 1 minute to attain the new setpoint (see Fig. 18). This may indicate that a certain minimum discharge power level is required (this probably provides additional heating to the insert) in order to allow the emitted current to increase.

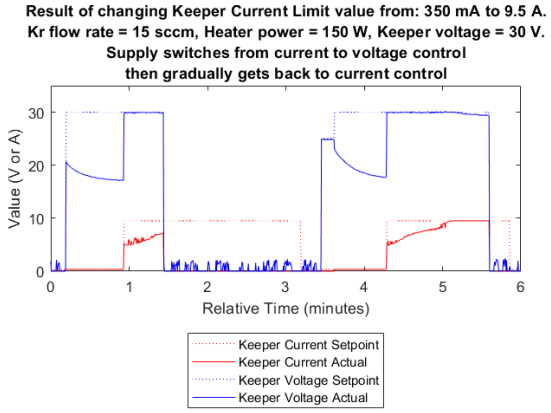

Figure 18. Hollow cathode is ignited with a 350 mA current limit which is then increased to 9.5 A. With a keeper voltage of 30 V the supply is able to regain current control mode at the higher discharge current.

The discharge heating power is minimal whilst at the 350 mA limit (17 V x 0.35 A = 6 W). When the keeper current limit is raised to 9.5 A the heating powers are approximately (27 V x 4 A = 108 W) and (30 V x 5 A = 150 W) for the two keeper voltage cases. Provided that the keeper supply can raise its voltage enough (and therefore provide sufficient heating power to the insert; between 108 W and 150 W in the example above) there appears to be no problem in transitioning from the low-power starting mode to normal, higher power operation.

6. CONCLUSION

Careful measurements have been made of the pre-ignition current in an LaB_6 hollow cathode with krypton gas. The measured current values span from 100's of nA up to several mA. At least 1 mA of pre-ignition current is present prior to ignition, however, it is also possible to obtain higher pre-ignition currents without igniting (for example if keeper voltage is insufficient). Pre-ignition currents are found to be conform to Child-Langmuir behaviour indicating that vacuum and pre-ignition currents are space charge limited. Pre-ignition current measurements may, in future, prove useful for monitoring of emitter condition, without even needing to ignite the hollow cathode.

Measurements of the current occurring during ignition have also been made. Ignition in Kr is found to be dependent upon mass flow rate, heater power and keeper voltage. Increasing the mass flow rate lowers the requirement for heater power and keeper voltage. The current that is reached after ignition is primarily determined by the power supply current limit and on first sight appears to yield current densities that considerably exceed the space charge limit calculated using Child's law. In fact, current density probably remains well below the space charge limit due to significant changes in the emission mechanism upon ignition. In order for this to be so, several of the relevant dimensions (i.e. effective emitter area, and electrode separation d) must therefore change significantly during ignition. For example, the relevant value for d may change from the electrode separation to the sheath thickness at the emitter surface.

Additionally, we report ignition of the hollow cathode at low mass flow rates of Kr, and low currents. Starting the cathode in this manner potentially reduces the insert and orifice erosion that occurs during ignition; however, this requires further experimental verification. We have demonstrated that, once ignited in this low power mode it is possible to migrate back to typical, higher power, operating conditions.

7. REFERENCES

1. I. Katz, I. G. Mikellides, D. M. Goebel, and J. E. Polk, "Insert Heating and Ignition in Inert-Gas Hollow Cathodes," *IEEE Transactions on Plasma Science*, vol. 36, pp. 2199-2206, 2008.
2. J. E. Polk, D. Goebel, P. Guerrero, "Thermal Characteristics of a Lanthanum Hexaboride Hollow Cathode," *Proceedings of the 34th International Electric Propulsion Conference, Hyogo, Japan, 2015*, unpublished, Paper No. IEPC-2015-044, 2015.
3. B. Rubin and J. D. Williams, "Hollow cathode conditioning and discharge initiation", *Journal of Applied Physics* 104, 053302, 2008.
4. W. G. Tighe, K. Chien, D. M. Goebel, and R. T. Longo, Hollow Cathode Emission and Ignition Studies at L-3 ETI," *Proceedings of the 30th International Electric Propulsion Conference, Florence, Italy, 2007*, unpublished, Paper No. IEPC-2007-023, 2007.
5. T. P. Lin and G. H. Eng, "Thermionic Emission Including both Space-Charge and Image Forces," *Journal of Applied Physics,* vol. 65, pp. 3205-3211, 1989.
6. J. B. Scott, "Extension of Langmuir Space-Charge Theory into the Accelerating Field Range," *Journal of Applied Physics*, vol. 52, pp. 4406-4410, 1981.
7. D. M. Goebel and I. Katz, *Fundamentals of Electric Propulsion: Ion and Hall Thrusters*: Wiley, 2008.
8. J. M. Lafferty, "Boride Cathodes," *Journal of Applied Physics,* vol. 22, pp. 299-309, 1951.
9. E. K. Storms and B. A. Mueller, "A study of surface stoichiometry and thermionic emission using LaB6," *Journal of Applied Physics*, vol. 50, pp. 3691-3698, 1979.

8. ACKNOWLEDGEMENT

We gratefully acknowledge Mars Space Ltd. For supply of the hollow cathode device and for support during these experiments.